

Electric quadrupole moment of the $5d^2D_{3/2}$ state in $^{171}\text{Yb}^+$: A relativistic coupled-cluster analysis

K. V. P. Latha^{1,*}, C. Sur^{1,2,†} and R. K. Chaudhuri¹, B. P. Das¹ and D. Mukherjee³

¹*Non-Accelerator Particle Physics Group, Indian Institute of Astrophysics, Bangalore - 560 034, India*

²*Department of Astronomy, The Ohio State University, Columbus, Ohio, 43210, USA and*

³*Department of Physical Chemistry, Indian Association for the Cultivation of Science, Kolkata - 700 032, India*

(Dated: Last revision : August 15, 2007 : 12:55 hrs : CS)

The electric quadrupole moment for the $5d^2D_{3/2}$ state of $^{171}\text{Yb}^+$, has been calculated using the relativistic coupled-cluster method. Earlier a similar calculation was performed for the $4d^2D_{5/2}$ state of $^{88}\text{Sr}^+$ which is the most accurate determination to date [PRL, **96**, 193001 (2006)]. The present calculation of the electric quadrupole moment of $^{171}\text{Yb}^+$ yielded a value $2.157ea_0^2$ where the experimental value is $2.08(11)ea_0^2$; a_0 is the Bohr radius and e the elementary charge. We discuss in this paper our results in detail for $^{171}\text{Yb}^+$ and highlight the dominant correlation effects present. We have presented the effect of inner core excitations and their contribution to the electric quadrupole moment, which is a property sensitive to regions away from the nucleus.

PACS numbers: 31.15.Ar, 31.15.Dv, 32.30.Jc

I. INTRODUCTION

The frequency of any periodic event like the mechanical oscillation of pendulum or stable atomic frequencies can be used to define the unit of time. The frequencies derived from selected atomic resonant transitions are particularly preferred due to various advantages they offer compared to mechanical oscillations. They are extremely stable, accurately measurable and reproducible. Though the cesium atomic clock frequency [1, 2] is accurate to 4 parts in 10^{16} , a variety of atoms and ions have been proposed as candidates for the next generation of frequency standards [3, 4]. Of these candidates, certain ions with forbidden transitions in the optical regime are of special importance. Trapped and laser cooled single ions and neutral atoms trapped in optical lattices are currently the leading candidates for atomic clocks [5, 6]. Frequency standard experiments with trapped ions require considerable skill and ingenuity. It is indeed very challenging to measure the clock frequencies to a high degree of precision. Effects like the second-order Zeeman, the electric quadrupole shift, etc. arise from the interaction of the ion with stray fields. It was shown recently that the systematic effects caused by these shifts will not limit the accuracy of the optical clock [7].

It was shown earlier that Yb^+ is one of the suitable candidates for defining a frequency standard [8, 9]. Other candidates like Sr^+ [10, 11], Ca^+ [12], Ba^+ [13], Hg^+ [5] etc have also been considered for setting up the frequency standard. In particular, Yb^+ is a very versatile candidate, having the clock transitions in the visible, IR and microwave regions. The transition which is being considered for the frequency standard experiment is the forbidden electric quadrupole ($E2$) transition between the

ground state ($6s^2S_{1/2}, F = 0$) and the metastable excited state ($5d^2D_{3/2}, F = 2$). Precise measurements of the electric quadrupole moments of these ions have been performed [7, 8, 9, 14, 15]. Comparison of the experimental values of electric quadrupole moments with those calculated theoretically, would serve as excellent tests of relativistic atomic theories. An earlier calculation of this quantity for Sr^+ , using relativistic coupled-cluster theory yielded a value $(2.94 \pm 0.07)ea_0^2$ [16] for the $4d^2D_{5/2}$ state, which was in very good agreement with its measured value (2.6 ± 0.3) [14], where e is the electronic charge and a_0 is the Bohr radius. This was the most accurate calculation of the quantity for the $4d^2D_{5/2}$ state of Sr^+ to date and the excellent agreement of the measured and the calculated values indicates the potential of the method used. In this paper, the electric quadrupole moment of Yb^+ in the state $5d^2D_{3/2}$ has been calculated using relativistic coupled-cluster (RCC) theory. Indeed a comparison of this property of a heavy ion like Yb^+ with accurate experimental data is a far more stringent test of RCC than the corresponding comparison for Sr^+ . The calculation of EQM for Yb^+ is computationally more demanding due to the presence of a large number of occupied orbitals. In our calculation, the entire core has been excited. This leads to a rapid proliferation in the number of cluster amplitude equations with the size of the virtual space considered, and therefore a very large increase in the number of computations necessary to determine these amplitudes. Obtaining convergence for the large number of cluster amplitude equations with an appropriate iterative method is a daunting task for heavy atomic systems like Yb^+ . The calculations on such systems hence involve the combination of the power of the relativistic many-body theories with the state-of-the-art high performance computational techniques.

An outline of the application of the RCC method to calculate atomic electric quadrupole moments has already been presented in [16]. The details of this theory have been discussed in several papers [17, 18]. Here we

*Electronic address: latha@iiap.res.in

†Electronic address: csur@astronomy.ohio-state.edu

shall give the salient features of the method for completeness. This paper is organized as follows : Section II and Section III deal with the theoretical methods we have employed and the details of our calculation respectively. In Section IV we present our results and compare with the available data. We have also discussed the effects of different many-body contributions. Finally we conclude in Section V and highlight the important findings of our work.

II. THEORETICAL METHODS

A. Relativistic coupled-cluster theory for closed shell atoms

We start with the N -electron closed-shell Dirac-Fock (DF) reference state $|\Phi\rangle$, which is the Fermi vacuum for the present formulation. In coupled-cluster (CC) theory the exact wavefunction for the core sector in terms of this reference state is given by,

$$|\Psi\rangle = \exp(T) |\Phi\rangle, \quad (1)$$

where T is the cluster operator which takes into account the excitations from the closed-shell core to the virtual orbitals. In singles and doubles (SD) approximation, the cluster amplitude T is written as

$$T = T_1 + T_2 = \sum_{ap} \{a_p^\dagger a_a\} t_a^p + \frac{1}{4} \sum_{abpq} \{a_p^\dagger a_q^\dagger a_b a_a\} t_{ab}^{pq}, \quad (2)$$

T_1 and T_2 being the cluster amplitudes for single and double excitations respectively and the curly brackets denote the *normal* ordering with respect to the Fermi vacuum. This is known as coupled-cluster with singles and doubles, namely CCSD. Here t_a^p and t_{ab}^{pq} are the corresponding single particle amplitudes and $a, b, \dots (p, q, \dots)$ stand for occupied (virtual) orbitals and $\{\dots\}$ denotes normal ordering with respect to the common reference state (vacuum) $|\Phi\rangle$. For a one-valence one-dimensional model space the label ‘v’ is used to represent a valence orbital. In our approach we deal with the normal ordered Hamiltonian which is defined as

$$\mathcal{H} \equiv H - \langle \Phi | H | \Phi \rangle = H - E_{DF}, \quad (3)$$

where E_{DF} is the Dirac-Fock energy.

B. Open shell coupled-cluster theory for single valence system : Electron Attachment (OSCC-EA)

To determine the wavefunctions for the open shell orbitals we employ open-shell coupled-cluster method for electron attachment (OSCC-EA) for the valence particle ($0h, 1p$) sector. Using the scheme of electron attachment

(EA) we obtain the $(N+1)$ -electron open shell system as

$$\text{Atom}(0,0) + e \longrightarrow \text{Ion}(0,1). \quad (4)$$

For a single valence system, we start with the reference state

$$|\Phi_v^{N+1}\rangle \equiv a_v^\dagger |\Phi\rangle \quad (5)$$

where v denotes the valence orbital as mentioned in the previous section and the operator a_v^\dagger represents creation of a particle in the valence space. The many-body exact open-shell wavefunction for the $(N+1)$ -electron open shell system now becomes,

$$|\Psi_v^{N+1}\rangle = \exp(T) \{\exp(S_v)\} |\Phi_v^{N+1}\rangle, \quad (6)$$

where the curly brackets denote the *normal* ordering with respect to $|\Phi\rangle$. For a single valence system, the operator $\exp(S_v)$ turns out to be $(1 + S_v)$

$$|\Psi_v^{N+1}\rangle = \exp(T) \{(1 + S_v)\} |\Phi_v^{N+1}\rangle, \quad (7)$$

with

$$S_v = S_{1v} + S_{2v} = \sum_{v \neq p} \{a_p^\dagger a_v\} s_v^p + \frac{1}{2} \sum_{bpq} \{a_p^\dagger a_q^\dagger a_b a_v\} s_{vb}^{pq}. \quad (8)$$

Here S_v corresponds to the excitation operator in the valence (v) sector and s_v^p and s_{vb}^{pq} are the singles and doubles amplitudes respectively. The evaluation of the cluster amplitudes are discussed elsewhere [?]. Apart from singles and doubles, only approximate triple excitations (CCSD(T)) have been included. In this calculation, we have used OSCC-EA to obtain the $5d^2 D_{3/2}$ state of $^{171}\text{Yb}^+$ which is followed by property calculations as given in sub-section II C.

C. Calculation of Expectation values

The expectation value of any operator O with respect to the exact state is given by

$$\begin{aligned} \langle O \rangle &= \frac{\langle \Psi^{N+1} | O | \Psi^{N+1} \rangle}{\langle \Psi^{N+1} | \Psi^{N+1} \rangle} \\ &= \frac{\langle \Phi^{N+1} | \{1 + S^\dagger\} \bar{O} \{1 + S\} | \Phi^{N+1} \rangle}{\langle \Phi^{N+1} | \{1 + S^\dagger\} \exp(T^\dagger) \exp(T) \{1 + S\} | \Phi^{N+1} \rangle} \quad (9) \end{aligned}$$

where $\bar{O} = \exp(T_c^\dagger) O \exp(T_c)$ is the dressed operator. The first few terms of the operators in the above expression (Eq. (9)) can be identified as \bar{O} , $\bar{O}S_1$, $\bar{O}S_2$,

$S_1^\dagger \bar{O} S_1$ etc. The corresponding matrix elements are referred to as dressed Dirac-Fock (DDF), dressed pair correlation (DPC) and dressed core polarization (DCP) respectively. We use the term ‘dressed’ because the operator \bar{O} includes the effects of certain core excitations, i.e., core-correlation effects. In addition to the above, we can identify a few other terms which play a non-negligible role in determining the correlation effects. One of those terms is $S_1^\dagger \bar{O} S_1 + c.c$ which we call the dressed higher order pair correlation (DHOPC) since it directly involves the correlation between a pair of electrons. Diagrams representing these terms have already been presented in ref. [16] but we have nevertheless given them here for clarity.

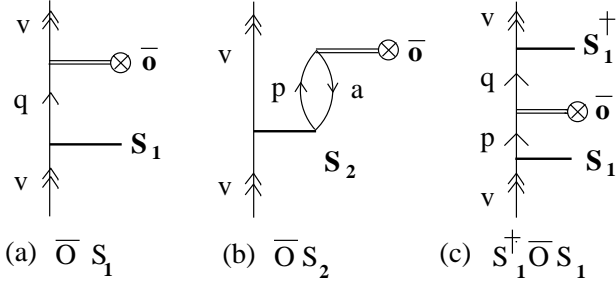


Figure 1: The diagrams (a) and (c) are subsets of dressed pair correlation (DPC) diagrams. Diagram (b) is one of the direct dressed core-polarization (DCP) diagram.

D. Electric Quadrupole Moment

The interaction of the atomic quadrupole moment with the external electric-field gradient is analogous to the interaction of a nuclear quadrupole moment with the electric fields generated by the atomic electrons at the nucleus. In the presence of the electric field, this gives rise to an energy shift by coupling with the gradient of the electric field. Thus the treatment of atomic electric quadrupole moment is analogous to its nuclear counterpart.

The quadrupole moment Θ of an atomic state $|\Psi(\gamma, J, M)\rangle$ is defined as the diagonal matrix element of the quadrupole operator with the maximum value M_J and is expressed as

$$\Theta = \langle \Psi(\gamma J F M_F) | \Theta_{zz} | \Psi(\gamma J F M_F) \rangle. \quad (10)$$

Here γ specifies the electronic configuration of the atoms which distinguishes the initial and final states; J is the total angular momentum of the atom and F is the summation of nuclear and atomic angular momentum with M_F its projection. The electric quadrupole operator in terms of the electronic coordinates is given by,

$$\Theta_{zz} = -\frac{e}{2} \sum_j (3z_j^2 - r_j^2),$$

where the sum is over all the electrons and z is the co-ordinate of the j th electron. To calculate the quantity we express the quadrupole operator in its single particle form as

$$\Theta_m^{(2)} = \sum_m q_m^{(2)} \quad (11)$$

and the single particle reduced matrix element is expressed as [19]

$$\langle j_f || q_m^{(2)} || j_i \rangle = \langle j_f || C_m^{(2)} || j_i \rangle \int dr r^2 (\mathcal{P}_f \mathcal{P}_i + \mathcal{Q}_f \mathcal{Q}_i). \quad (12)$$

In Eq. (12), the subscripts f and i correspond to the final and initial states respectively; \mathcal{P} and \mathcal{Q} are the radial part of the large and small components of the single particle Dirac-Fock wavefunctions respectively and j_i is the total angular momentum for the i th electron. The angular factor is given by

$$\langle j_f || C_m^{(k)} || j_i \rangle = (-1)^{(j_f+1/2)} \sqrt{(2j_f+1)} \sqrt{(2j_i+1)} \times \begin{pmatrix} j_f & 2 & j_i \\ -1/2 & 0 & 1/2 \end{pmatrix} \pi(l, k, l') \quad (13)$$

where

$$\pi(l, k, l') = \begin{cases} 1 & \text{if } l + k + l' \text{ even} \\ 0 & \text{otherwise} \end{cases}$$

l and k being the orbital angular momentum and the rank respectively.

Finally using the Wigner Eckart theorem we define the electric quadrupole moment in terms of the reduced matrix elements as

$$\langle j_f | \Theta_m^{(2)} | j_i \rangle = (-1)^{j_f - m_f} \begin{pmatrix} j_f & 2 & j_i \\ -m_f & 0 & m_f \end{pmatrix} \langle j_f || \Theta^{(2)} || j_i \rangle \quad (14)$$

III. COMPUTATIONAL DETAILS

This calculation is performed in the following steps : The first step being the generation of single particle basis for Yb^{++} using the Gaussian basis set expansion. This is followed by the generation of the coupled cluster amplitudes (T) for the closed-shell Yb^{++} system. In the next step, the virtual orbitals $6s$ and $5d_{3/2}$ are generated using the open-shell coupled cluster method for electron attachment (OSCC-EA). This is followed by the property calculations as given in subsection II C.

The orbitals used in the present work are generated by kinetically balanced finite basis set expansion (FSBE) of Gaussian type orbitals (GTO) [20]

$$F_{i,k}(r) = r^k \exp(-\alpha_i r^2), \quad (15)$$

with $k = 0, 1, 2, \dots$ for s, p, d, \dots type functions, respectively. The exponents are determined by the even tempering condition [21]

$$\alpha_i = \alpha_0 \beta^{i-1}. \quad (16)$$

The starting point of the computation is the generation of the Dirac-Fock (DF) orbitals [20] which are defined on a radial grid of the form

$$r_i = r_0 [\exp(i-1)h - 1] \quad (17)$$

with the freedom of choosing the parameters r_0 and h . All DF orbitals are generated using a two parameter Fermi nuclear distribution

$$\rho = \frac{\rho_0}{1 + \exp((r-c)/a)}, \quad (18)$$

where the parameter c is the half charge radius and a is related to skin thickness, defined as the interval of the nuclear thickness in which the nuclear charge density falls from near one to near zero. Table I contains the information about the basis functions used in the calculation to determine the electric quadrupole moment of $5d^2D_{3/2}$ state of $^{171}\text{Yb}^+$.

Table I: No. of basis (NB) functions used to generate the even tempered Dirac-Fock orbitals and the corresponding value of $\alpha_0 = \alpha \times 10^{-5}$ and β used. NP and NH stand for number or particles and number of holes respectively.

	$s_{1/2}$	$p_{1/2}$	$p_{3/2}$	$d_{3/2}$	$d_{5/2}$	$f_{5/2}$	$f_{7/2}$	$g_{7/2}$	$g_{9/2}$
NB	38	35	35	25	25	25	25	20	20
α	305	325	325	335	335	315	315	345	345
β	2.106	2.116	2.116	2.316	2.316	2.216	2.216	2.135	2.135
NP	7	8	8	7	7	7	7	8	8
NH	5	4	4	2	2	1	1	0	0

IV. RESULTS AND DISCUSSION

The contribution of the important physical effects to the electric quadrupole moment of $^{171}\text{Yb}^+$ is given in Table II. The total value that we have obtained for this quantity $\Theta_{3/2}(\text{calculated}) = 2.157ea_0^2$ is within the error bounds of the measured value $\Theta_{3/2}(\text{measured}) = (2.08 \pm 0.11)ea_0^2$ [9]. It would be instructive to compare our present calculation based on the RCC theory with a previous calculation performed by Itano using the relativistic configuration interaction (RCI) method [22]. The value obtained by Itano is $\Theta_{3/2} = 2.174ea_0^2$ [22]. The RCI calculation of Itano uses a multiconfiguration Dirac-Fock (MCDF) extended optimized level (EOL) orbital basis. The configurations included in the latter calculation constitute a subset of the configurations in our calculation. In particular, they correspond to the correlation effects arising from the single and double excitations from the core and the valence, i.e., terms involving T_1 , T_2 , S_1 and S_2 in our RCC calculation. In

our calculation, the above effects have been included to all orders. The virtual orbitals considered by Itano were $\{(6-10)s, (6-10)p, (6-10)d, (5-7)f, (5-6)g, 6h\}$. The calculation carried out by Itano involves 2 main steps. In the first step, the SPOs are obtained by minimizing an energy functional in a limited orbital space in the framework of MCDF-EOL. The second step involves a fairly large RCI calculation to account for the correlation effects. Itano's calculation incorporates the valence-core correlation (single and the double excitations) arising from the $\{5d\}$ and $\{4f, 5s, 5p\}$ shells and single excitations from $\{4s, 4p, 4d, 3d\}$ (core-core correlations). In spite of these differences, the results are in good agreement.

For each symmetry we have considered more virtual orbitals than Itano. In addition, we have considered single and double excitations from all the core orbitals where Itano has considered only single and double excitations from $5d$ and $\{4f, 5s, 5p\}$ core orbitals, but not more than one single core excitation at a time.

From Table II, we see that the dressed Dirac-Fock contribution is the largest and it is a substantial fraction of the total EQM, in spite of the large number of core-valence excitations. The second largest contribution is from the DPC effects and third being DCP effects. DPC effects arise from the terms like $\bar{O}S_1$ and $S_1^\dagger \bar{O}S_1$. Subsection II C gives the details of these different many-body terms. S_1 is an operator of rank 0 and the valence orbital in $^{171}\text{Yb}^+$ is a $5d_{3/2}$ orbital and hence it excites the valence electron to a virtual orbital of the same parity and angular momentum giving a large contribution through the virtual d orbitals. Clearly the effects of the valence $5d_{3/2}$ excitations are the most important in the case of $^{171}\text{Yb}^+$. It is interesting to note that though $^{171}\text{Yb}^+$ has more filled shells than for $^{88}\text{Sr}^+$, the contribution of the DDF, DPC, DCP terms follow the same trend for $^{171}\text{Yb}^+$ and $^{88}\text{Sr}^+$. The core-virtual electric quadrupole excitations/deexcitations contributing to the DCP diagrams involve excitations from f - f or d - d or f - p , etc orbitals. The DCP diagrams involve the contributions from the \bar{O} and the S_2 matrix elements. Though the \bar{O} matrix element could be large in some cases, the contribution of the matrix element of the product $\bar{O}S_2$ turns out to be two orders of magnitude smaller than that of the DDF term, in spite of the possibility of large number of core-virtual excitations. Similar trends were observed for the EQM of $^{88}\text{Sr}^+$. Table I has more details about the virtual orbitals and the active space. From Table II, we find that the contributions of the terms DDF, DPC, DCP and DHOPC to the final value are 119%, -14%, -2.2%, 1.2% respectively for $^{88}\text{Sr}^+$ and are 116%, -13.3%, -1.3%, 1.34 % respectively for $^{171}\text{Yb}^+$. Also, the total contribution of DPC, DCP and DHOPC to DDF is -1.1 %. DPC is $\sim 11\%$ of the DDF. DCP is $\sim 1\%$ of DDF for the case of $^{171}\text{Yb}^+$. It has been observed that this trend is similar for $^{88}\text{Sr}^+$ even though $^{171}\text{Yb}^+$ has a larger core.

Table II: Contributions from the electric quadrupole moment (in ea_0^2) of the $5d^2D_{3/2}$ state of $^{171}\text{Yb}^+$ and the $4d^2D_{5/2}$ state of $^{88}\text{Sr}^+$, corresponding to different many-body effects in the CCSD calculation. The terms like DDF, DCP, DPC, DHOPC are explained in the text.

Ion	DDF	DPC	DCP	DHOPC	Total	Expt. [9]
Yb^+	2.500	-0.287	-0.0280	0.029	2.157	2.08 ± 0.11
Sr^+	3.496	-0.4306	-0.0642	0.0353	2.94	2.6 ± 0.3

V. CONCLUSIONS

In summary, we have used relativistic coupled-cluster theory to calculate the electric quadrupole moments (EQM) of the $5d^2D_{3/2}$ state of $^{171}\text{Yb}^+$. Our determi-

nation of EQM of the $5d^2D_{3/2}$ state of $^{171}\text{Yb}^+$ is within the experimental limits. It highlights the ability of RCC to capture the interplay between the relativistic and the correlation effects in heavy single valence ions. We have also determined the various leading many-body effects arising in this calculation. To our knowledge this calculation yields the most accurate theoretical value of EQM of the $5d^2D_{3/2}$ state of $^{171}\text{Yb}^+$ to date. It is a useful theoretical supplement to the experimental search for optical frequency standards.

Acknowledgments

This work is partially supported by BRNS project no. 2002/37/12/BRNS. RKC acknowledges the Department of Science and Technology, India (grant SR/S1/PC-32/2005).

-
- [1] R. Wynands and S. Wyers, *Metrologia*, **42**, S64 (2005).
 - [2] <http://tf.nist.gov/cesium/atomichistory.htm>
 - [3] H.S. Margolis, *et al.*, Atomic Phys. **20**, Proceedings XX, ICAP, 2006. Published by AIP Conference Preceedings, 869.
 - [4] L. Hollberg *et al.*, *J. Phys. B* **38**, S469 (2005).
 - [5] W. H. Oskay *et al.*, *Phys. Rev. Lett.*, **97**, 020801 (2006).
 - [6] M. Takamoto, F-L Hong, R. Higashi, H. Katori, *Nature* **435**, 321 (2005).
 - [7] W. H. Oskay, W. M. Itano and J. C. Bergquist, *Phys. Rev. Lett.* **94**, 163001 (2005).
 - [8] J. Stenger *et al.*, *Opt. Lett.* **26**, 1589 (2001).
 - [9] T. Schneider, E. Pein, and C. Tamm, *Phys. Rev. Lett.* **94**, 230801 (2005).
 - [10] J. E. Bernard *et al.*, *Phys. Rev. Lett.* **82**, 3228 (1999).
 - [11] H. S. Margolis *et al.*, *Phys. Rev. A* **67**, 032501 (2003).
 - [12] C. Champenois *et al.*, *Phys. Lett. A* **331**, 298 (2004).
 - [13] J. A. Sherman *et al.*, *Phys. Rev. Lett.* **94**, 243001 (2005).
 - [14] G. P. Barwood *et al.*, *Phys. Rev. Lett.* **93**, 133001 (2004).
 - [15] P. Dube *et al.*, *Phys. Rev. Lett.* **95**, 033001 (2005).
 - [16] C. Sur *et al.*, *Phys. Rev. Lett.* **96**, 193001 (2006).
 - [17] R. F. Bishop, Lecture Notes in Physics, *Microscopic Quantum Many-Body Theories and their Applications*, p.1, Eds. J. Navarro and A. Polls, Springer-Verlag-Berlin, Heidelberg and New York (1998).
 - [18] R. J. Bartlett, *Modern Electronic Structure Theory*, vol-II, p.1047, Ed. D. R. Yarkony, World Scientific, Singapore (1995).
 - [19] I. P. Grant, *J. Phys. B*, **7**, 1458 (1974).
 - [20] R. K. Chaudhuri, P. K. Panda and B. P. Das, *Phys. Rev. A*, **59**, 1187 (1999).
 - [21] R. C. Raffanetti and K. Ruedenberg, *J. Chem. Phys.*, **59**, 5978 (1973).
 - [22] Wayne M. Itano, *Phys. Rev. A*, **73**, 022510 (2006).